Single-crystal Magnetic Properties of Lanthanide Complexes. Part X.[1] Hexakis(antipyrine)holmium(III) Tri-iodide

By **M. Gerloch** * and **D. J. Mackey**, University Chemical Laboratory, Lensfield Road, Cambridge CB2 1EW

The principal and average magnetic moments of hexakis(antipyrine)holmium(III) tri-iodide [antipyrine (antip) is 2,3-dimethyl-1-phenyl-Δ^3-pyrazolin-5-one] have been measured in the temperature range 80—300 K. The results are interpreted within a point-charge crystal-field model of D_{3h} symmetry by use of $^5/_8$ and $^5/_7$ free-ion states as basis, corrected for the effects of intermediate coupling. A range of values for ρ_4 and ρ_6, the fourth- and sixth-order radial parameters, is fixed for $Ho(antip)_6I_3$ by the temperature-dependence of mean moments. For points within this range, anisotropies fix values of $A_2^{\circ}\langle r^2\rangle$, related to the coefficient of the second-order crystal-field harmonic. Intermediate compromise values are: $\rho_4 = 350$, $\rho_6 = 150$, $A_2^{\circ}\langle r^2\rangle = 220$ cm^{-1}.

We describe the magnetic properties of single crystals of the f^{10} holmium analogue of the trigonally distorted octahedral[2] series $Ln(antip)_6I_3$ [where (antip) is antipyrine = 2,3-dimethyl-1-phenyl-Δ^3-pyrazolin-5-one]. Crozier and Runciman[3,4] have fitted baricentres of

[1] Part IX, M. Gerloch and D. J. Mackey, *J.C.S. Dalton*, 1972, 415.

[2] R. W. Baker and J. W. Jeffery, *Acta Cryst.*, 1969, *A*, XIV, 16 (Stony Brook Internat. Union Cryst. Abs., 1969); R. W. Baker, personal communication.

[3] M. H. Crozier and W. A. Runciman, *J. Chem. Phys.*, 1961, **35**, 1392.

[4] M. H. Crozier and W. A. Runciman, *J. Chem. Phys.*, 1962, **36**, 1088.

holmium compound spectra [5-8] to a free-ion, intermediate-coupling model parameterized by the three energies E_1, E_2, and E_3 as interelectron repulsion factors and ζ, the spin–orbit coupling coefficient. Their papers quote best-fit parameters, spin–orbit matrices, calculated eigenvalues, and percentage purities of the eigenvectors. The eigenvectors proper were not quoted and we therefore do so in the Appendix, having constructed them by repeating their calculations. The mean observed energy levels and purities of the lowest states for f^{10} are given in Table 1.

TABLE 1

Energies and purities of lowest states of f^{10} free ions

State	$^5I_8$	$^5I_7$	$^5I_6$	$^5I_5$	$^5I_4$	$^5F_4$
Energy/cm^{-1}	0	5120	8590	11,218	13,319	15,510
Purity (%)	93	97	95	91	90	82

Our crystal-field calculations have again employed the model described in Part I.[9] The Ho(antip)$_6^{3+}$ complex ion lies at a crystal site of symmetry $\bar{3}$; the ' octahedra ' are centrosymmetric and suffer a general angular distortion with respect to the unique crystal c axis. We have chosen to reduce the large number of variables a freely parameterized model requires in the following empirical way. We follow the common practice of assuming that the crystal-field effects of the organic ligands can be approximated by nearest-neighbour interactions alone, thus defining these interactions to be directed along the Ho–O bonds or along some closely related ' effective ' bond axes directed at the metal atom. This assumption then raises the symmetry from S_6 to D_{3d} so effecting some reduction in the number of free parameters. Representation of these effects by point-charges rather than point-dipoles directed toward the central metal is then a relatively unimportant choice. We have opted for the point-charge approach for reasons of simplicity in calculation and in comparing our results with others throughout the lanthanide and transition series. Within this empirical point-charge model of D_{3d} symmetry we use the usual parameters [9] ρ_2, ρ_4, and ρ_6, being radial integrals associated with second-, fourth-, and sixth-order terms in the crystal-field potential. The angle θ between the unique crystal axis and any Ho–O vector then describes the angular distortion of the ion. We refer to θ as the ' distortion angle,' remembering, however, that $\theta = \theta_{oct} = \cos^{-1}\sqrt{\frac{1}{3}}$ for the case of zero distortion from a regular octahedral array of point-charges. Insofar that we represent the antipyrine ligands by point-charges, the angle θ is to be regarded as an ' effective ' parameter of the system and not simply defined by the M–O vectors as defined by X-ray analysis.[2] Our model also assumes that this empirically defined θ parameter also satisfactorily takes up errors introduced by neglecting any dipolar contributions normal to the metal–ligand bonds. Finally, the great bulk of the six antipyrine ligands presumably ensures the assumption of magnetic dilution is valid.

Calculations have been performed by use of $^5I_8 + {}^5I_7$ states as basis, corrected for the effects of intermediate coupling as in the Appendix, and so involved diagonalization of a 32 × 32 matrix.

EXPERIMENTAL

Powder susceptibilities and crystal anisotropies of Ho(antip)$_6$I$_3$ were measured in the temperature range 80—300 K by the Gouy and Krishnan ' critical torque ' methods, respectively. The results, corrected for the diamagnetic properties of the lutetium analogue,[9] are given in Tables 2 and 3: interpolated values of principal molecular magnetic moments appear in Table 4. Procedures and calibrations are as in ref. 10.

TABLE 2

Experimental average magnetic susceptibilities of Ho(antip)$_6$I$_3$

T/K	$10^6\bar{\chi}_M'$ / c.g.s.u. mol^{-1}	T/K	$10^6\bar{\chi}_M'$ / c.g.s.u. mol^{-1}
302·5	45,280	194·5	70,170
293·5	46,820	173·5	78,160
288·0	47,880	162·0	83,530
276·0	49,590	146·0	92,570
267·5	51,090	131·0	102,350
261·5	52,380	114·0	116,450
238·5	57,170	99·5	132,950
214·0	63,790	91·0	146,150

TABLE 3

Experimental magnetic anisotropies of Ho(antip)$_6$I$_3$

T/K	$10^6(\chi_\parallel - \chi_\perp)$ / c.g.s.u. mol^{-1}	T/K	$10^6(\chi_\parallel - \chi_\perp)$ / c.g.s.u. mol^{-1}
295·5	7350	182·5	20,000
281·0	8335	179·0	20,670
259·5	9705	157·0	25,710
247·0	11,070	144·5	29,070
227·0	13,110	132·5	32,870
210·5	15,270	118·5	37,800
191·0	18,240	97·5	48,760
		86·5	55,140

DISCUSSION

Energy levels of an f^{10} ion in six-co-ordinate D_{3d} symmetry are shown for the lowest state $^5I_8$ as functions of distortion angle θ in Figure 1. There is an E_g ground state except for θ between *ca.* 60 and 63° when an A_{2g} state crosses it to become the lowest-energy state. Between 58 and 65°, these two levels remain within 2 cm^{-1} of each other. Although there is always an E_g ground state for trigonal elongation ($\theta < \theta_{oct}$) a second E_g level remains fairly close to ground and at θ *ca.* 50° approaches within 3·8 cm^{-1} of it.

Despite this behaviour of energy levels, the principal and average magnetic moments in Figure 2 show ' normal ' behaviour with θ, as compared with those for other members of this series. The magnetic anisotropy

[5] H. Gobrecht, *Ann. Phys.*, 1937, **28**, 673.
[6] G. Rosenthal, *Phys. Z.*, 1959, **40**, 5.
[7] H. Severin, *Z. Physik*, 1949, **125**, 455.
[8] H. G. Kahle, *Z. Physik*, 1956, **145**, 347.
[9] Part I, M. Gerloch and D. J. Mackey, *J. Chem. Soc.* (*A*), 1970, 3030.
[10] B. N. Figgis, M. Gerloch, J. Lewis, and R. C. Slade, *J. Chem. Soc.* (*A*), 1968, 2028.

is in the sense $\mu_{\parallel} > \mu_{\perp}$ for $\theta < \theta_{oct}$. The mean moments, $\bar{\mu}$ (300 K) and $\bar{\mu}$ (100 K), are independent of θ and, not shown, of ρ_2. In one respect, however, the moments shown in Figure 2 are anomalous in that the magnitudes

TABLE 4

Interpolated principal magnetic moments of $Ho(antip)_6I_3$

T/K	$\bar{\mu}$/B.M.	$\mu_{\parallel}$/B.M.	$\mu_{\perp}$/B.M.
302·5	10·47	11·01	10·20
293·5	10·49	11·03	10·21
288·0	10·51	11·06	10·22
276·0	10·47	11·05	10·17
267·5	10·46	11·06	10·15
261·5	10·47	11·11	10·13
238·5	10·45	11·15	10·08
214·0	10·45	11·23	10·04
194·5	10·45	11·30	10·00
173·5	10·42	11·36	9·93
162·0	10·41	11·36	9·90
146·0	10·40	11·42	9·86
131·0	10·36	11·43	9·79
114·0	10·31	11·43	9·70
99·5	10·29	11·44	9·67
91·0	10·32	11·48	9·68

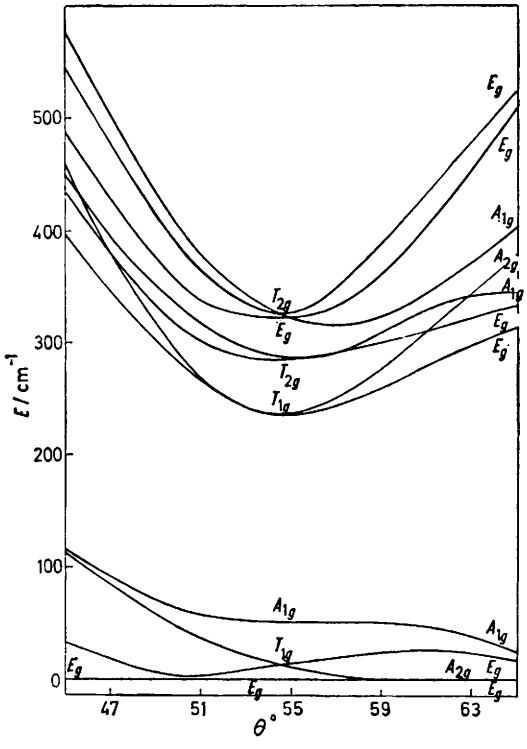

FIGURE 1 Energy levels arising in D_{3d} crystal field from free-ion $^5I_8$ state of f^{10} configuration as functions of θ; $\rho_2 = 1500$, $\rho_4 = 500$, $\rho_6 = 300$ cm^{-1}

of magnetic anisotropies and of the temperature variations of both $\Delta\mu$ and $\bar{\mu}$ are fairly small in relation to the size of $\bar{\mu}$. It will be interesting, therefore, to see how well the same point-charge model used throughout this series can reproduce the experimental values for $Ho(antip)_6I_3$.

The dependences of principal and average moments on the fourth- and sixth-order radial parameters ρ_4 and ρ_6 are shown in Figures 3(a) and (b) respectively. Mean moments decrease a little with increasing ρ_4 and ρ_6 about equally at 300 K; rather more with ρ_6 at 100 K.

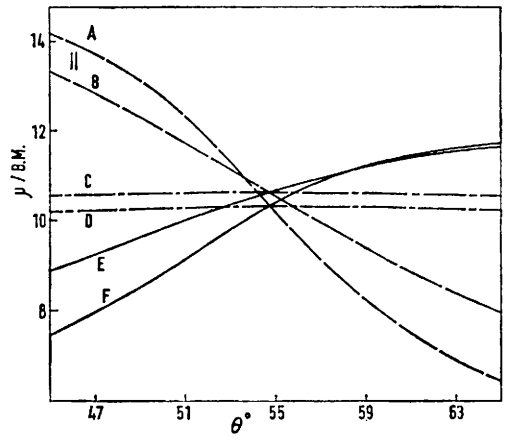

FIGURE 2 Principal and average magnetic moments for f^{10} system as functions of θ and temperature; $\rho_2 = 1500$, $\rho_4 = 500$, $\rho_6 = 300$ cm^{-1}; A and B, $\mu_{\parallel}$ at 100 and 300 K respectively; C and D, $\bar{\mu}$ at 300 and 100 K respectively; E and F, $\mu_{\perp}$ at 300 and 100 K respectively

Anisotropies behave differently with respect to the two parameters, $\Delta\mu$ decreasing with increasing ρ_4 or decreasing ρ_6. The curves in Figure 3 are appropriate for the conditions quoted, *viz.*, $\rho_6 = 300$ cm^{-1} in 3(a) and $\rho_4 = 400$ cm^{-1} in 3(b). From similar graphs, not shown, we observe, however, that the behaviour of values with respect to ρ_4 depends upon ρ_6 and *vice versa*. Thus, for ρ_6 *ca.* 600 cm^{-1}, $\bar{\mu}$ (100 K) is independent of ρ_4 (200—1200 cm^{-1}). Further $\bar{\mu}$ (300 K) is generally fairly insensitive to ρ_4 or ρ_6. We find, in consequence, that we

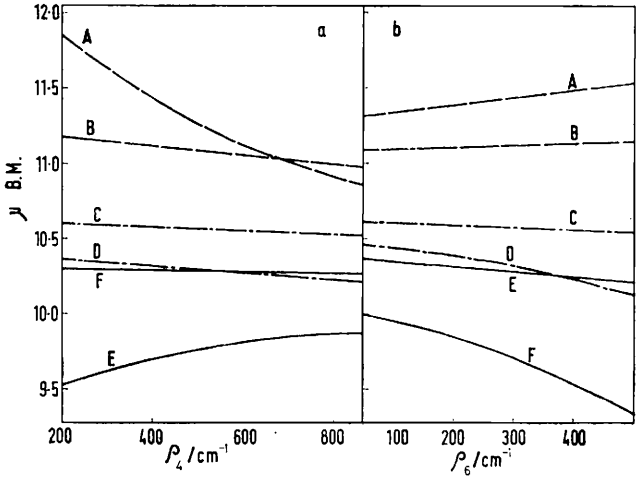

FIGURE 3 Principal and average magnetic moments for f^{10} ions as functions of (a) ρ_4, when $\rho_2 = 1500$, $\rho_6 = 300$ cm^{-1}, $\theta = 53°$ and (b) ρ_6, when $\rho_2 = 1500$, $\rho_4 = 400$ cm^{-1}, and $\theta = 53°$; curves A—F as in Figure 2

can fit the $\bar{\mu}$ values for $Ho(antip)_6I_3$ within 1% (experimental error) anywhere in the ranges: $200 < \rho_4 < 1200$ cm^{-1}, $0 < \rho_6 < 600$ cm^{-1}. This unsatisfactory situation

is greatly improved, however, if we examine the temperature-dependence of $\bar{\mu}$, for which the experimental error is considerably less.

In Figure 4 we plot calculated values of $\bar{\mu}$ (300) — $\bar{\mu}$ (100) as functions of ρ_4 for a family of ρ_6 values. The experimental value for Ho(antip)$_6$I$_3$ shown with an estimated error of $\pm$0·01 B.M. is the *difference* between mean moments at the two temperatures. It is fortunate to find an experimental value for $\bar{\mu}$ (300) — $\bar{\mu}$ (100) as low as 0·16 B.M. for this immediately sets limits on ρ_4 and ρ_6: a value near 0·35 B.M., for example, could not. The possible ρ_4 and ρ_6 values are fixed very much more sensitively than by consideration of the absolute $\bar{\mu}$ values alone. ρ_4 Must be less than *ca.* 500 cm^{-1} and $\rho_6 \leqslant 200$

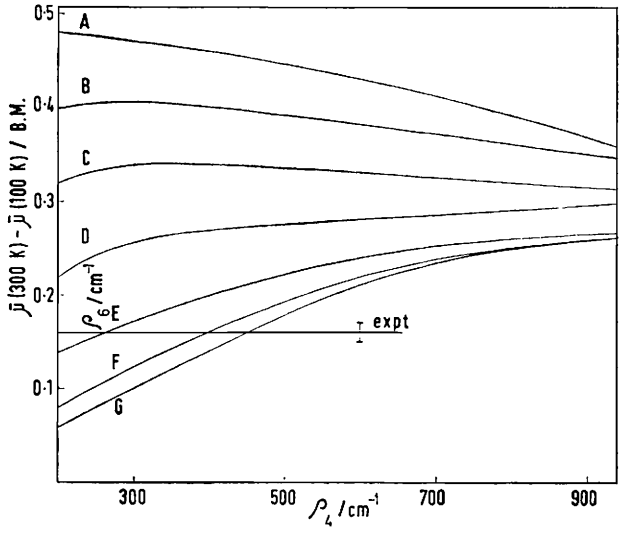

FIGURE 4 Calculated temperature dependence of $\bar{\mu}$ as function of ρ_4 and ρ_6. Experimental value of $\bar{\mu}$ (300 K) — $\bar{\mu}$ (100 K) for Ho(antip)$_6$I$_3$ is shown with error bar of $\pm$0·01 B.M.; ρ_6 = A, 600; B, 500; C, 400; D, 300; E, 200; F, 100; and G, 50 cm^{-1}

cm^{-1}, but there is an inverse correlation between these parameter values. An intermediate choice might be $\rho_4 = 350$, $\rho_6 = 150$ cm^{-1}. In what follows we shall consider two cases representing situations near the extreme ends of the fits shown in Figure 4, *viz.*, $\rho_4 = 450$, $\rho_6 = 50$ cm^{-1}, and $\rho_4 = 250$, $\rho_6 = 200$ cm^{-1}.

For each of these two cases we have calculated anisotropies as functions of ρ_2 and θ in the usual way.[1] In anticipation of the result we note the point made in Figure 3 that the dependences of $\Delta\mu$ on ρ_4 and ρ_6 are opposed, so there will tend to be a cancellation effect such that $A_2^{\circ}\langle r^2\rangle$ values [9] for the two cases should not be *too* different. Tables 5(a) and (b) list for various ρ_2 values, θ values which exactly fit $\Delta\mu$ of Ho(antip)$_6$I$_3$ at 300, 200, and 100 K with associated $A_2^{\circ}\langle r^2\rangle$ values for each case. Also shown are calculated $\bar{\mu}$ values which are invariably *ca.* 1% greater than the observed values, *i.e.*, within experimental error. As for other members of the series θ^f, the θ value to fit, varies a little with temperature and the dependence of θ^f on temperature is slightly different for the two cases studied. As predicted from the general trends noted earlier, $A_2^{\circ}\langle r^2\rangle$ values for the two cases are somewhat similar being *ca.* 25% greater for $\rho_4 = 450$, $\rho_6 = 50$ cm^{-1}.

TABLE 5

Ho(antip)$_6$I$_3$. ρ_2/θ Values to fit anisotropies: calculated $A_2^{\circ}\langle r^2\rangle$ [$= \frac{3}{2}\rho_2(3\cos^2\theta - 1)$] and $\bar{\mu}$ values

Experimental values of $\bar{\mu}$: 300 K, 10·48; 200 K, 10·44; 100 K, 10·33 B.M.

T/K	θ°	$A_2^{\circ}\langle r^2\rangle$/cm^{-1}	$\bar{\mu}$ (calc)/B.M.
(a) $\rho_4 = 450$; $\rho_6 = 50$ cm^{-1}			
$\rho_2 = 500$ cm^{-1}			
300	49·48	200	10·60
200	48·60	234	10·56
100	48·75	228	10·44
$\rho_2 = 1000$ cm^{-1}			
300	51·83	219	10·60
200	51·31	258	10·56
100	51·17	270	10·43
$\rho_2 = 1500$ cm^{-1}			
300	52·80	217	10·60
200	52·38	268	10·56
100	52·23	281	10·43
$\rho_2 = 2000$ cm^{-1}			
300	53·25	222	10·60
200	52·93	271	10·56
100	52·79	292	10·43
(b) $\rho_4 = 250$; $\rho_6 = 200$ cm^{-1}			
$\rho_2 = 500$ cm^{-1}			
300	50·43	163	10·60
200	50·27	170	10·57
100	51·42	125	10·44
$\rho_2 = 1000$ cm^{-1}			
300	52·30	182	10·60
200	52·12	197	10·57
100	52·62	158	10·44
$\rho_2 = 1500$ cm^{-1}			
300	53·10	183	10·61
200	52·89	208	10·57
100	53·17	176	10·45
$\rho_2 = 2000$ cm^{-1}			
300	53·45	193	10·61
200	53·32	210	10·57
100	53·53	181	10·45

In conclusion we quote values for Ho(antip)$_6$I$_3$ as lying between the correlated sets: $\rho_4 = 450$, $\rho_6 = 50$, and $A_2^{\circ}\langle r^2\rangle = 260 \pm 35$ cm^{-1}; and $\rho_4 = 250$, $\rho_6 = 200$, and $A_2^{\circ}\langle r^2\rangle = 190 \pm 30$ cm^{-1}. A compromise set would be $\rho_4 = 350$, $\rho_6 = 150$, and $A_2^{\circ}\langle r^2\rangle$ *ca.* 220 cm^{-1}. As will be discussed at the conclusion of this series, these values fall in line with those of the holmium analogues so that the same point-charge model appears to describe the magnetic properties adequately even for the somewhat anomalously low anisotropies and temperature variations for f^{10} noted in Figure 2.

APPENDIX

Using the matrices and best-fit, intermediate-coupling parameters of Crozier and Runciman,[3,4] we have calculated the diagonalization of the free-ion f^{10} states.

Eigenvectors for the lowest states are as in Table 6 where [11,12] in ${}^{a}_{b}X_{c}$, ${}^{a}X$ is a Russell–Saunders term label, b is the seniority number, and c is the Racah U quantum number. Correction factors [13] by which the crystal-field reduced matrix elements used in conjunction with pure Russell–Saunders state functions must be multiplied have been calculated from the eigenvectors above. They are as in Table 7.

TABLE 6

$$^5I_8 = 0{\cdot}9665|^5{}_4I_{20}\rangle + 0{\cdot}1189|^3{}_4K_{21}\rangle - 0{\cdot}2221|^3{}_4K_{30}\rangle - 0{\cdot}0326|^3{}_4L_{21}\rangle + 0{\cdot}0110|^1{}_4L_{21}\rangle + 0{\cdot}0333|^1{}_4L_{22}\rangle - 0{\cdot}0065|^3{}_4M_{30}\rangle$$

$$^5I_7 = 0{\cdot}9852|^5{}_4I_{20}\rangle + 0{\cdot}0381|^3{}_4I_{20}\rangle - 0{\cdot}0338|^3{}_4I_{30}\rangle + 0{\cdot}0730|^3{}_4K_{21}\rangle - 0{\cdot}1455|^3{}_4K_{30}\rangle - 0{\cdot}0063|^1{}_4K_{21}\rangle - 0{\cdot}0190|^3{}_4L_{21}\rangle$$

TABLE 7

$U2$ $U4$ $U6$	$^5I_8$	$^5I_7$
$^5I_8$	0·9141	
	0·9283	
	0·9386	
$^5I_7$	0·9063	0·9625
	0·9342	0·9711
	0·9414	0·9880

We thank the S.R.C. for a research grant (to D. J. M.).

[1/1664 *Received*, 10*th September*, 1971]

[11] B. G. Wybourne, ' Spectroscopic Properties of Rare Earths,' Interscience, New York, 1965.

[12] C. W. Nielson and C. F. Koster, ' Spectroscopic Coefficients for the p^n, d^n, and f^n Configurations,' M.I.T. Press, Cambridge, Mass., 1963.

[13] M. Gerloch and D. J. Mackey, *J. Chem. Soc.* (*A*), 1971, 3372.